

**HOT SPOT MECHANISM IN BUBBLE
SENSITIZED COMMERCIAL EXPLOSIVES**

**S.K. Chan, ICI Explosives
and
K.K. Feng, Canadian Explosives Research Laboratory**

Report Documentation Page				Form Approved OMB No. 0704-0188	
Public reporting burden for the collection of information is estimated to average 1 hour per response, including the time for reviewing instructions, searching existing data sources, gathering and maintaining the data needed, and completing and reviewing the collection of information. Send comments regarding this burden estimate or any other aspect of this collection of information, including suggestions for reducing this burden, to Washington Headquarters Services, Directorate for Information Operations and Reports, 1215 Jefferson Davis Highway, Suite 1204, Arlington VA 22202-4302. Respondents should be aware that notwithstanding any other provision of law, no person shall be subject to a penalty for failing to comply with a collection of information if it does not display a currently valid OMB control number.					
1. REPORT DATE AUG 1990		2. REPORT TYPE		3. DATES COVERED 00-00-1990 to 00-00-1990	
4. TITLE AND SUBTITLE Hot Spot Mechanism in Bubble Sensitized Commercial Explosives				5a. CONTRACT NUMBER	
				5b. GRANT NUMBER	
				5c. PROGRAM ELEMENT NUMBER	
6. AUTHOR(S)				5d. PROJECT NUMBER	
				5e. TASK NUMBER	
				5f. WORK UNIT NUMBER	
7. PERFORMING ORGANIZATION NAME(S) AND ADDRESS(ES) ICI Explosives,Beloeil Site, ,McMasterville, Quebec, Canada J3G 1T9,				8. PERFORMING ORGANIZATION REPORT NUMBER	
9. SPONSORING/MONITORING AGENCY NAME(S) AND ADDRESS(ES)				10. SPONSOR/MONITOR'S ACRONYM(S)	
				11. SPONSOR/MONITOR'S REPORT NUMBER(S)	
12. DISTRIBUTION/AVAILABILITY STATEMENT Approved for public release; distribution unlimited					
13. SUPPLEMENTARY NOTES See also ADA235006, Volume 2. Minutes of the Explosives Safety Seminar (24th) Held in St. Louis, MO on 28-30 August 1990.					
14. ABSTRACT see report					
15. SUBJECT TERMS					
16. SECURITY CLASSIFICATION OF:			17. LIMITATION OF ABSTRACT Same as Report (SAR)	18. NUMBER OF PAGES 22	19a. NAME OF RESPONSIBLE PERSON
a. REPORT unclassified	b. ABSTRACT unclassified	c. THIS PAGE unclassified			

HOT SPOT MECHANISM IN BUBBLE
SENSITIZED COMMERCIAL EXPLOSIVES

by

S.K. Chan
Senior Research Scientist,
ICI Explosives, Beloeil Site,
McMasterville, Quebec, Canada J3G 1T9

K.K. Feng
Head, Explosives Research,
Canadian Explosives Research Laboratory,
CANMET, Energy, Mines & Resources, Canada

ABSTRACT

Water-gels and emulsions exhibit two fundamental hot-spot mechanisms, namely shock heating of materials surrounding voids and adiabatic compression heating of bubble gases. By a comparison of the reaction kinetics derived from (a) VOD-diameter data using the recently developed computer code CPEX and (b) a reaction model proposed previously, it is shown that at the detonation regime, the dominant hot-spot mechanism is shock heating and the remaining explosive outside of the hot-spots is consumed by burning as proposed in the model. At the lower compression rates, the dominant initiation sensitization mechanism is the adiabatic compression of the gas in entrained bubbles. This is proven by the results from an experimental impact test on chemically sensitized water-gel explosive. The same mechanism operates in the DDT regime of these explosives. The time to ignition is shown to be related to the time of pressurization in both the impact test and the DDT tests.

INTRODUCTION

It is well known that explosive initiation sensitivity is significantly increased by the action of hot spots (1). However, the fundamental mechanisms of such hot spots are still a highly uncertain subject, particularly for a solid explosive. The number of possible hot spot mechanisms for the latter is extremely large involving mechanisms unique to solids (2) in addition to the commonly accepted ones for liquids, e.g. adiabatic compression of occluded gas voids (3) and shock heating (4). Water-gels and emulsions have characteristics of liquids, as far as initiation mechanisms are concerned. These much simpler mechanisms, which operate largely independently and at different ranges of initiation compression rates, allow a much easier understanding of the operation of the initiation mechanisms in these explosives, especially in the area of detonation. The latter has been successfully modelled by Chan (5,6). Recent development in detonation theory of non-ideal explosives (6,7) has produced an extremely powerful tool to deduce overall reaction rates from experimental detonation velocities at various charge diameters. This technique allows an independent check of the validity of reaction models proposed in Ref. 6. The two different reaction kinetics are compared in this paper.

At lower compression rates for water-gel and emulsion explosives, e.g. mechanical impact and pressurization due to internal ignition in confined or semi-confined medium such as in deflagration to detonation transition (DDT) events, hot spots are generated by the adiabatic compression of the gas pockets. This is related to the safety of the manufacturing and transport of such

explosives which has recently received much attention since the accidental explosion of emulsion explosive in a piston pump at the McMasterville site of C-I-L Inc. in 1988. This paper presents some previously unpublished data on the ASTM impact initiation and DDT of water-gel explosives which demonstrates the importance of adiabatic compression as a mechanism in such initiation mechanisms.

INITIATION UNDER DETONATION CONDITIONS

The experimental work of Campbell et al (8) and the theoretical work of Mader (4) have demonstrated convincingly that shock heating of materials surrounding the air bubbles is the most effective hot spot mechanism under shock initiation conditions such as those in the detonation wave. To demonstrate the shock heating effect quantitatively for liquids, shock temperatures of the materials upstream and downstream of a one-dimensional air-gap traversed by a plane shock wave (9) are shown in Fig. 1. In this Figure T_1 is the temperature of nitromethane heated by the shock wave from the initial temperature of T_0 , T_2 is the residual temperature after the material expands into the air-gap and T_3 is the temperature behind the reflected shock created in the upstream gap material after it impacts the opposite face of the air-gap. Mader's results for T_1 and T_3 are also shown in Fig.1. There is good agreement between the two sets of calculations. The results in Fig. 1 show clearly that under shock pressures of the order of 10 GPa, T_3 is almost 2700 K assuming an initial temperature of 293 K. The detonation shock causes the high temperature T_3 in the hot spot and instantaneously ignition follows.

The above shock void interaction hot spot mechanism was used

The above shock void interaction hot spot mechanism was used in the detonation models of References (5) and (6). The experimental detonation velocities were determined for a liquid explosive (EGMN/AN/EG/Water 50/25/20/5). The desired densities were obtained by mixing in glass microspheres (B15BX, 3M) (5). The recently developed I.C.I. slightly divergent flow computer code CPEX (7) is used here to re-analyze this data for the purpose of determining the reaction kinetics of the explosive. The theoretical fits to the VOD versus inverse charge diameter for three initial densities (1.1, 1.15, 1.2 kg/dm³) are shown in Figs. 2a-c. The CPEX deduced extent of reaction / time curves are shown in Fig. 3 for the three initial densities at a pressure of 5 GPa. The lower parts of these curves suggest that the extent of reaction of the hot spots, as indicated by the point of sharp change in slopes, correspond to the initial void volume fraction of 0.077, 0.115 and 0.154 for the three densities respectively. Beyond the hot spot volumes, the reaction curves resemble closely the theoretical grain burning curves of Ref. 6 as shown in Fig. 4. This can be taken as an independent confirmation of the validity of the grain burning model proposed in Ref. 6.

In the reaction model of Ref. 6, the hot spots were assumed to have an effective volume equal to $2^{1/2}/4$ of the initial void volume. The curves of Figs. 3 suggest that it should be equal to the void volume. Another assumption in this model was that the hot spots were to be initiated both by bulk thermal reaction and by burning instantaneously at the collapsed wall of the bubble by the hot compressed gas (see Fig. 5). However, the shape of the CPEX reaction curves in Fig. 3 in the hot spot reaction region indicates there is no grain burning reaction in this region. Otherwise, the

initial slopes of these curves should be higher than the slopes of the curves beyond these regions, instead of a gradually increasing slope. The hot spots with their higher temperature should have higher burning speed than the cooler material outside of the hot spots. In retrospect, this is not surprising. The glass microspheres are at very low pressure (typically about 0.1 atmosphere), which reduces the ability of the compressed gas to ignite the surrounding explosive. Furthermore, the glass wall material would absorb most of the gas energy. Thus the hot spot reaction in this case is reduced to one of thermal reaction in the shock heated hot spots in the explosive.

INITIATION UNDER IMPACT AND DDT CONDITIONS

When a gas bubble is present in a liquid explosive, including water gel and emulsions, the impact sensitivity is increased significantly (1). This makes the explosive more hazardous in the handling and manufacturing processes. In order to simulate the effect of gas bubbles on the impact sensitivity of such explosives, the ASTM Impact Test tool (10) shown in Fig.6 was used to test these explosives. About 30 mm³ of explosive is placed in the steel cup. An air space of 26 mm³ is formed in the centre of the O-ring under the stainless steel diaphragm. The cup assembly is positioned in the container body in direct contact with a roller bearing, which is connected to strain gauges for force measurement. The air space in the cup is precompressed to about 7 mm³. This tool was used to study the response of an EGMN based water-gel explosive. An impact weight of 5 kg was used. Positive results were obtained above a drop height of 0.36 m. The pressure record

from a positive test is shown in Fig. 7. The pressure increase following the initial impact pulse is attributed to the combustion of the explosive. There seems to be little doubt that the initiation mechanism is the ignition of the explosive by the hot compressed air.

Another hazard test carried out on the above EGMN based water-gel explosive was the DDT test. The test setup is shown schematically in Fig. 8. It consists of a heavy wall seamless steel tubing (19 mm ID/50.8 mm OD) with lengths of either 0.5 m or 0.9 m. An igniter is placed inside the closed end of the tube (11). The igniter compound used was either 2 g of RDX or RDX/black powder mixture. The outer wall of the steel tube at the igniter location was connected to strain gauges to monitor the pressure build-up history. A thin wall collapsible aluminum wave velocity probe was placed in the centre of the tube which was filled with the test explosive. Two EGMN based water-gel explosives which showed DDT behaviour were tested. These explosives (EXP-A contained 3% aluminum and EXP-B contained 7% of aluminum) had nominal density of 1.12 kg/dm^3 . These explosives were produced by chemical gassing, and contained small gas bubbles with nominal average diameter of $70 \text{ }\mu\text{m}$. The volume percent of air bubbles are 27 and 32% respectively for the two explosives. Figure 9 shows the igniter end pressure and wave velocity records for a test with EXP-A initiated with RDX/black powder igniter. The transition to detonation can be clearly seen from the wave velocity record which has a steady velocity of 0.77 km/s from the igniter to 0.58 m downstream at which it changes sharply to 4.25 km/s , corresponding to the detonation velocity of this explosive. The pressure reaches 0.45 GPa prior to a dramatic increase which seems to be the source

of the transition to detonation. If the trajectory of the detonation wave is extrapolated back to the igniter location, the time coincides with the moment of explosion in the pressure record. The initial pressurization rate was 490 GPa/s and the time from initiation of the igniter to the moment of the explosion is .640 ms (Fig. 9). A summary of other pressurization rate (normalized by the initial atmospheric pressure) and delay to explosion data is shown in Fig.10. There is a good correlation of these two parameters. The data from the impact test (Fig. 7) for EXP-A is also shown in the same figure. The impact data fits in very well with the DDT data indicating the close relationship between the two initiation events. This suggests that the DDT mechanism is the ignition of the explosive by the hot compressed bubble gas similar to that occurring in the impact test.

CONCLUSION

The results presented in this paper demonstrated the two basic hot-spot mechanisms in water-gel explosives. The shock heating of materials around voids is the dominant mechanism if shock initiation events involve a particle velocity above a few hundred meters per second. However, for more gentle pressurization, such as mechanical impact or combustion in a confined medium, the adiabatic compression of bubble gas becomes the more effective hot-spot mechanism. The presence of glass microspheres in an explosive is probably not effective for this latter mechanism since there is insufficient gas present in the microspheres and the glass would also absorb most of the gas energy to prevent transfer of heat to the explosive. This suggest that glass microsphere sensitized explosives are much safer in

compression events. However, there is always a danger of the presence of air pockets of volatile gases. Nevertheless, the hazards engineer should be aware of the potential hazards of manipulating such an apparently safe medium in rapid pressurization operations, despite the relative safety of the use of glass microspheres. For hazard quantification purposes, more work is still needed to quantify the ignition conditions.

REFERENCES

1. Bowden F.P. and Yoffe A.D., "Initiation and growth of explosion in liquids and solids", 1952, Cambridge University Press
2. Winter R.E. and Field J.E. "The role of localized plastic flow in the impact initiation of explosives", Proc. Roy. Soc. Lond. A. 343, 399-413 (1975).
3. Chaudhri M.M. and Field J.E. "The role of rapidly compressed gas pockets in the initiation of explosives", Proc. Roy. Soc., Vol. A340, 113-128 (1974).
4. Mader C.L., "Initiation of detonation by the interaction of shock with density discontinuities", Physics of Fluids, Vol. 8, 1811-1816, (1965).

5. Chan S.K., "A model for predicting the critical diameter of bubble sensitized explosives", Proceedings, Symposium H.D.P.: Behaviour of Dense Media Under High Dynamic Pressures, Paris, (1978), 233-244.
6. Chan S.K., "Theoretical prediction of the velocity-diameter relation of bubble-sensitized liquid explosives", Propellants, Explosives, Pyrotechnics, 8, 184-192 (1983).
7. Kirby I.J. and Leiper G.A., "A small divergent detonation theory for intermolecular explosives", Proceedings of the 8th Symposium (International) on Detonation, Albuquerque, p.176 (1985).
8. Campbell A.W., Davis W.C. and Travis J.R., "Shock initiation of detonation in liquid explosives", Phys. Fluids, 4 498-510, (1916).
9. Chan S.K., "A shock sensitivity model for aerated liquids", Report EL6810, (1976), Canadian Industries Limited, Montreal, Canada.
10. ASTM Standards ANSI/ASTM D 2540-70 (Reapproved 1980), "Standard Test Method for Drop Weight Sensitivity of Liquid Mono-propellants", American Society for Testing and Materials, Philadelphia, Pa., U.S.A.
11. Chan S.K. "Deflagration to detonation transition behaviour of water-gel explosives", C-I-L Inc. (now ICI Explosives, Canada), McMasterville, P.Q., Canada.

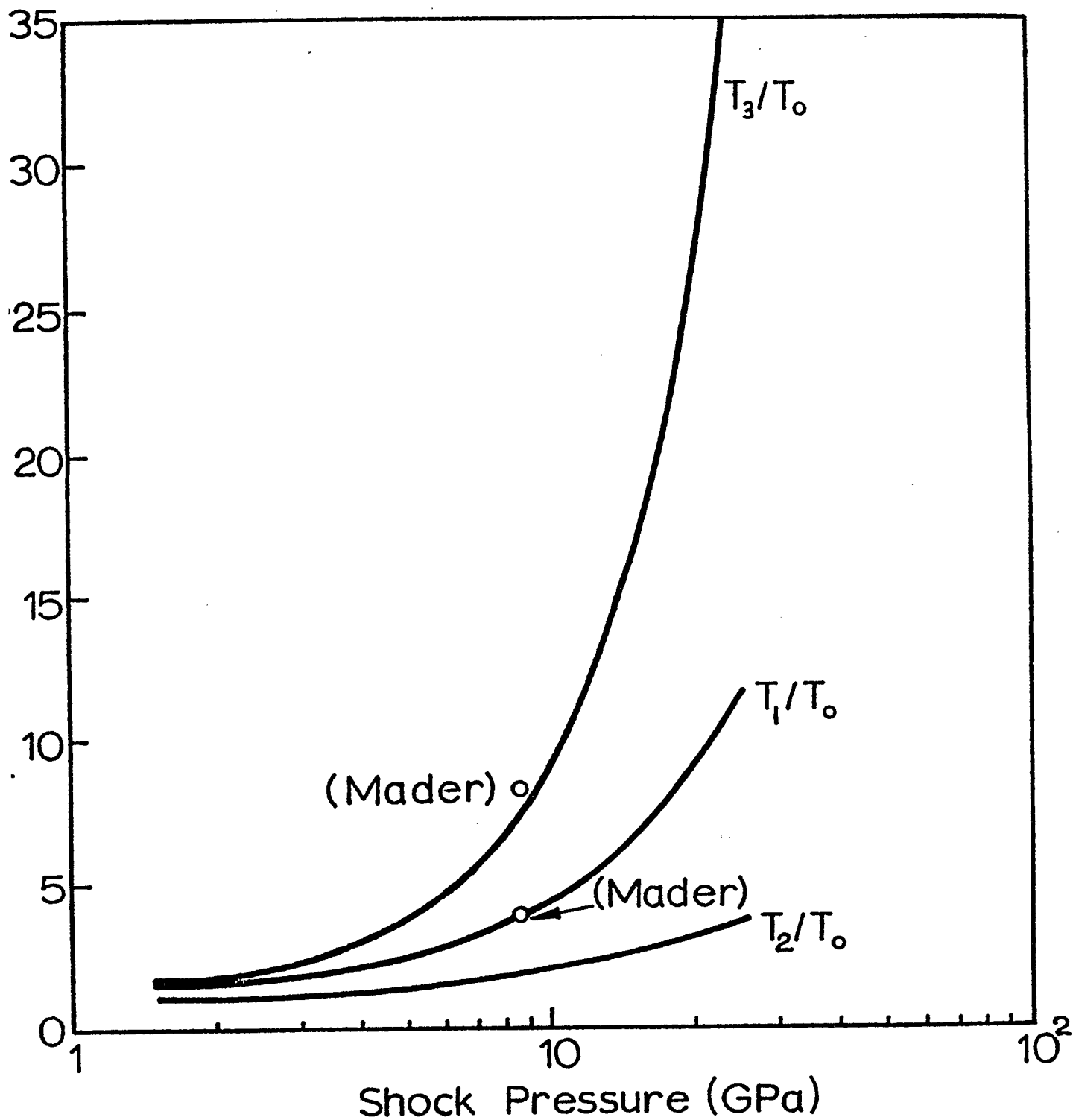


Figure 1, Shock temperature of nitromethane upstream and downstream of a one dimensional air-gap traversed by a plane shock wave.

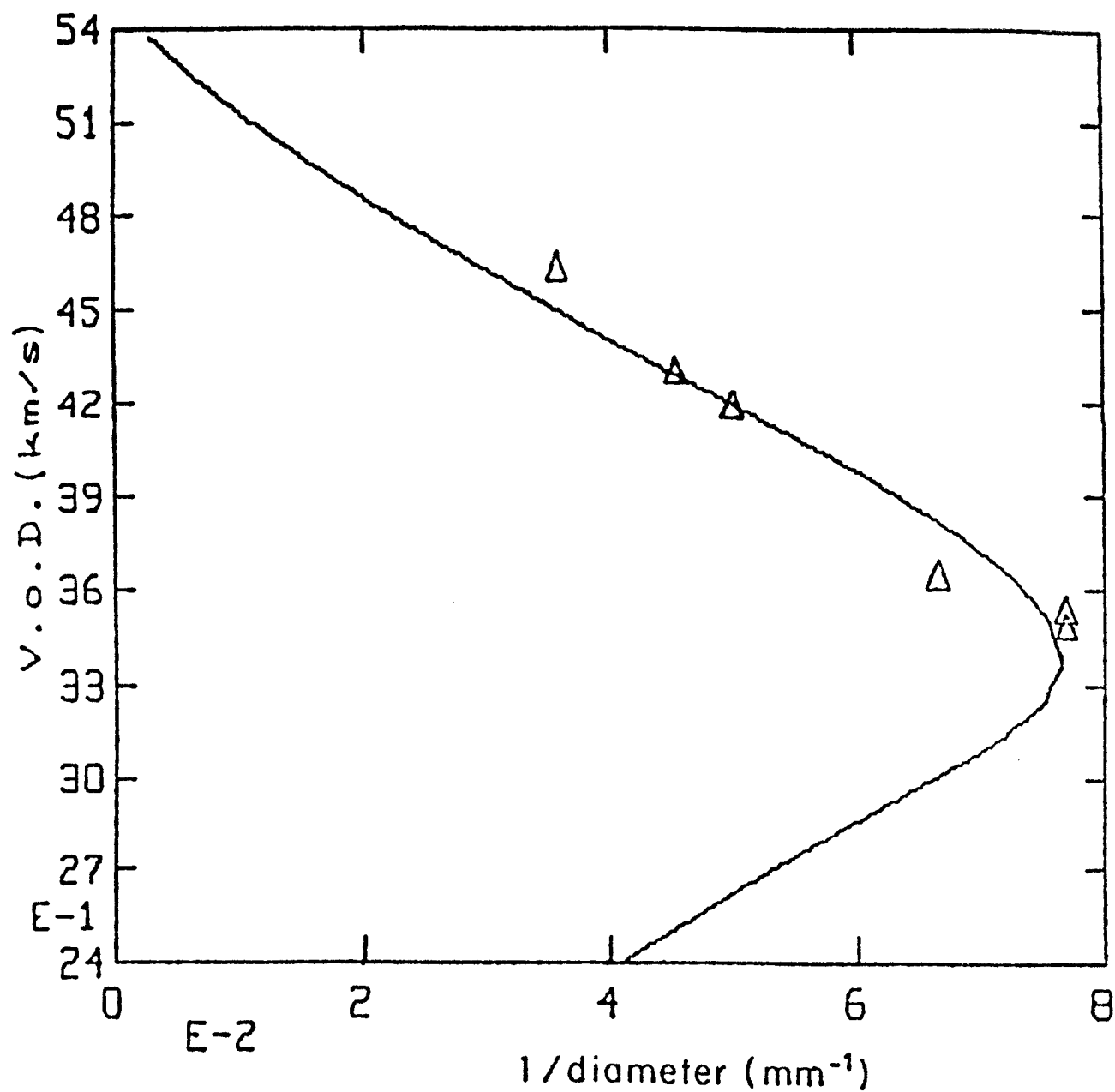


Figure 2a, Theoretical detonation velocity versus reciprocal charge diameter on 1.1 g/cm³ EGMN at unconfined condition.

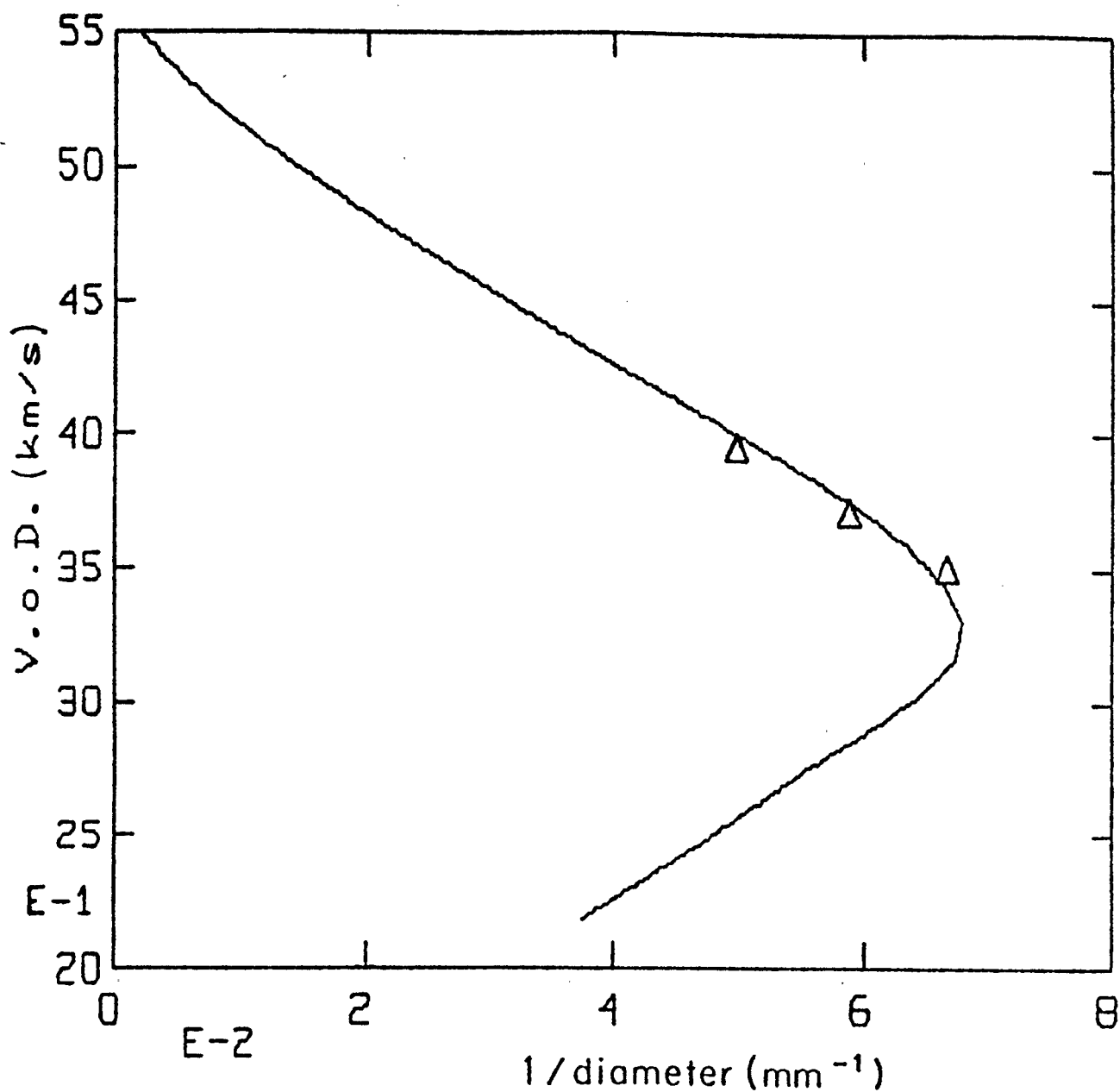


Figure 2b, Theoretical detonation velocity versus reciprocal charge diameter for 1.15 g/cm³ EGMN at unconfined conditions.

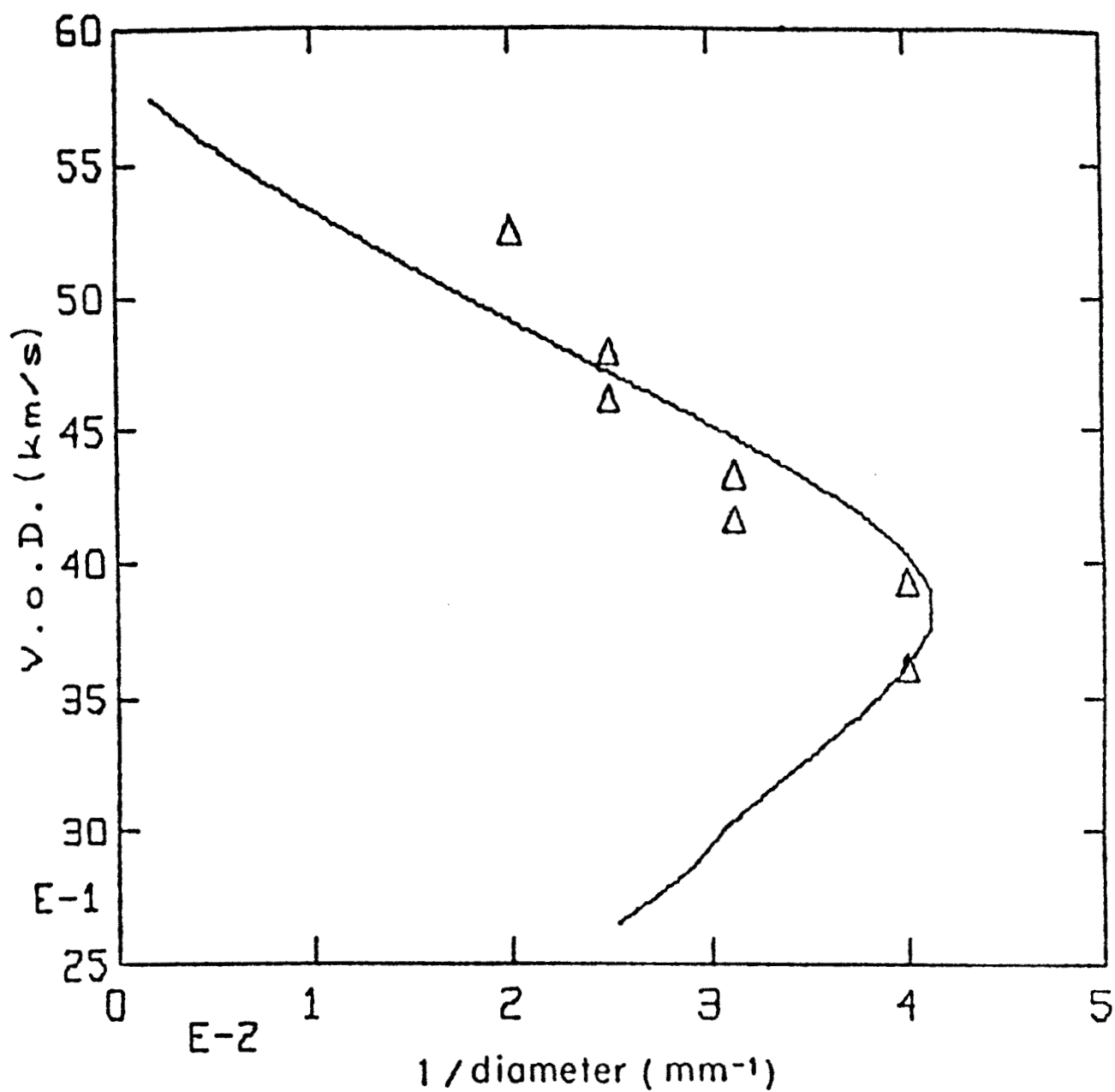


Figure 2c,

Theoretical detonation velocity versus reciprocal charge diameter for 1.2 g/cm³ EGMN at unconfined conditions.

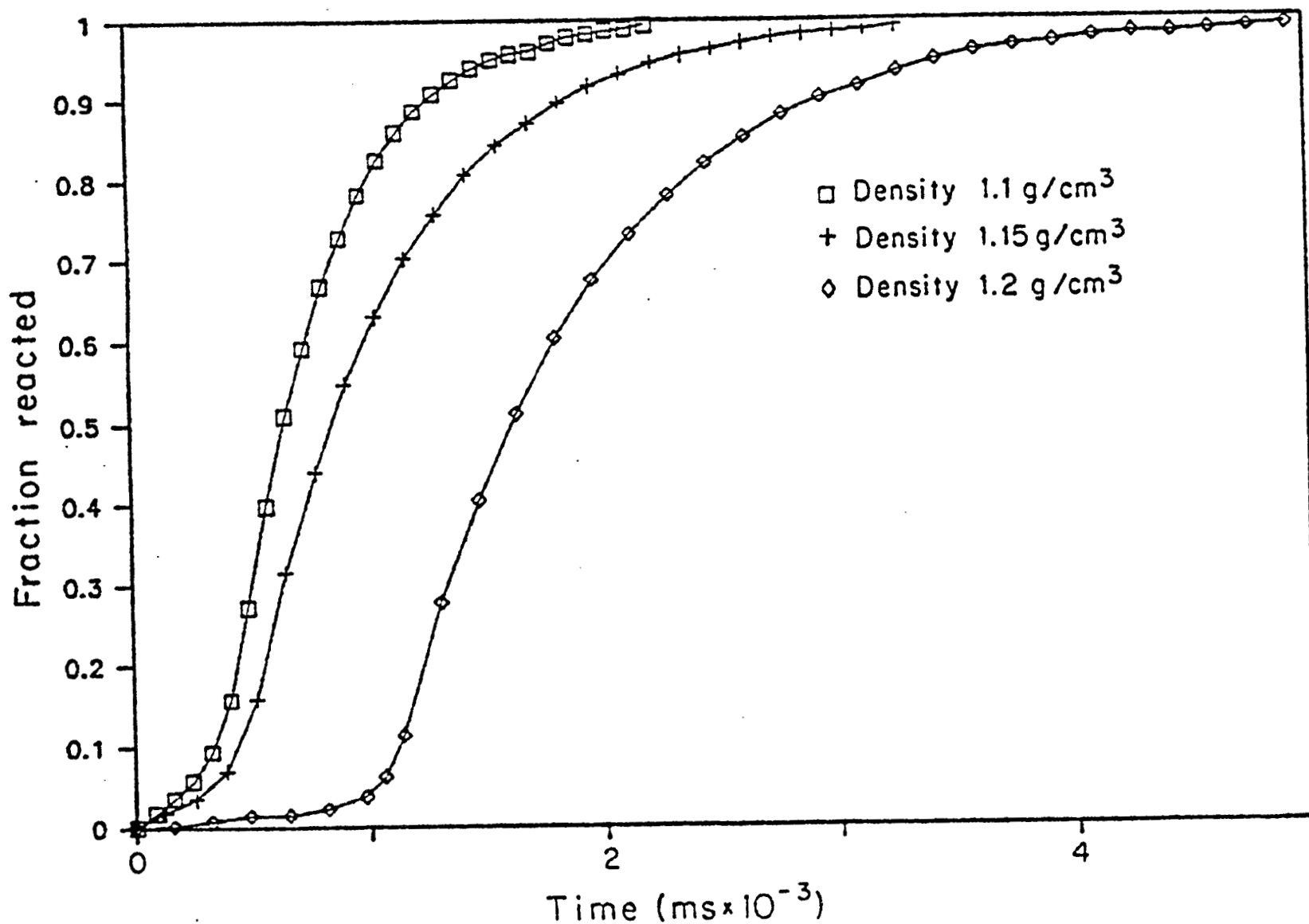


Figure 3, Fraction reacted vs. time curves for the initial densities (1.1, 1.15, 1.2 g/cm³) at a pressure of 5.0 GPa.

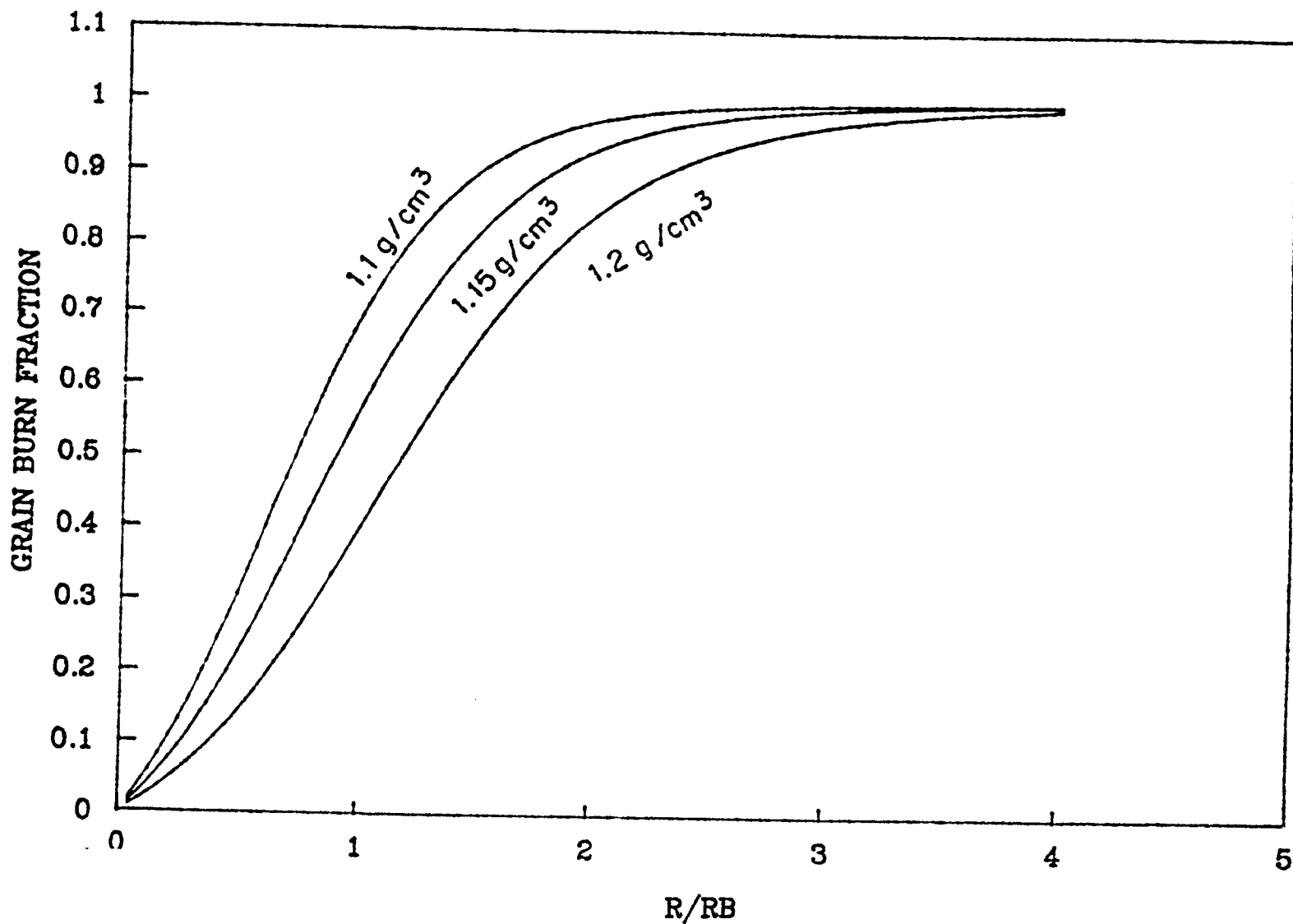


Figure 4, Comparison of the grain burn fraction versus flame propagation distance with the analytical fits for initial density of 1.1 g/cc, 1.15 g/cc and 1.2 g/cc.

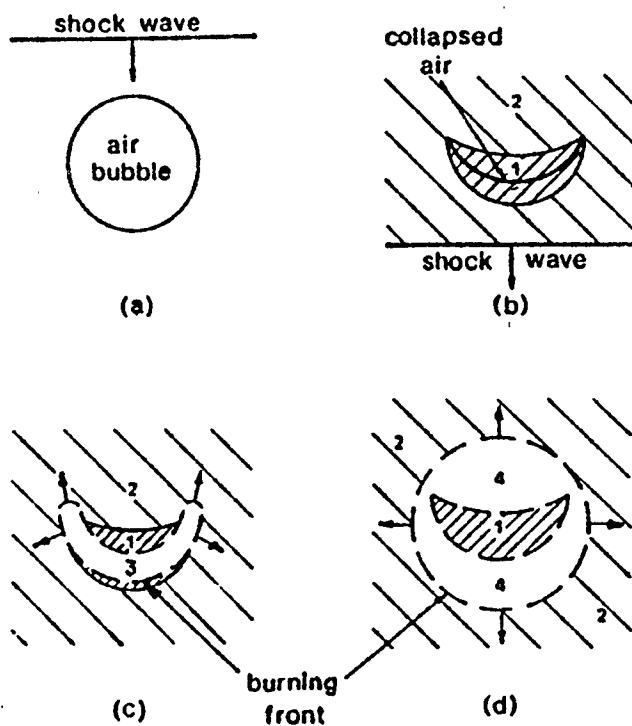


Figure 5, Schematic representation of the reaction behind the detonation shock wave.

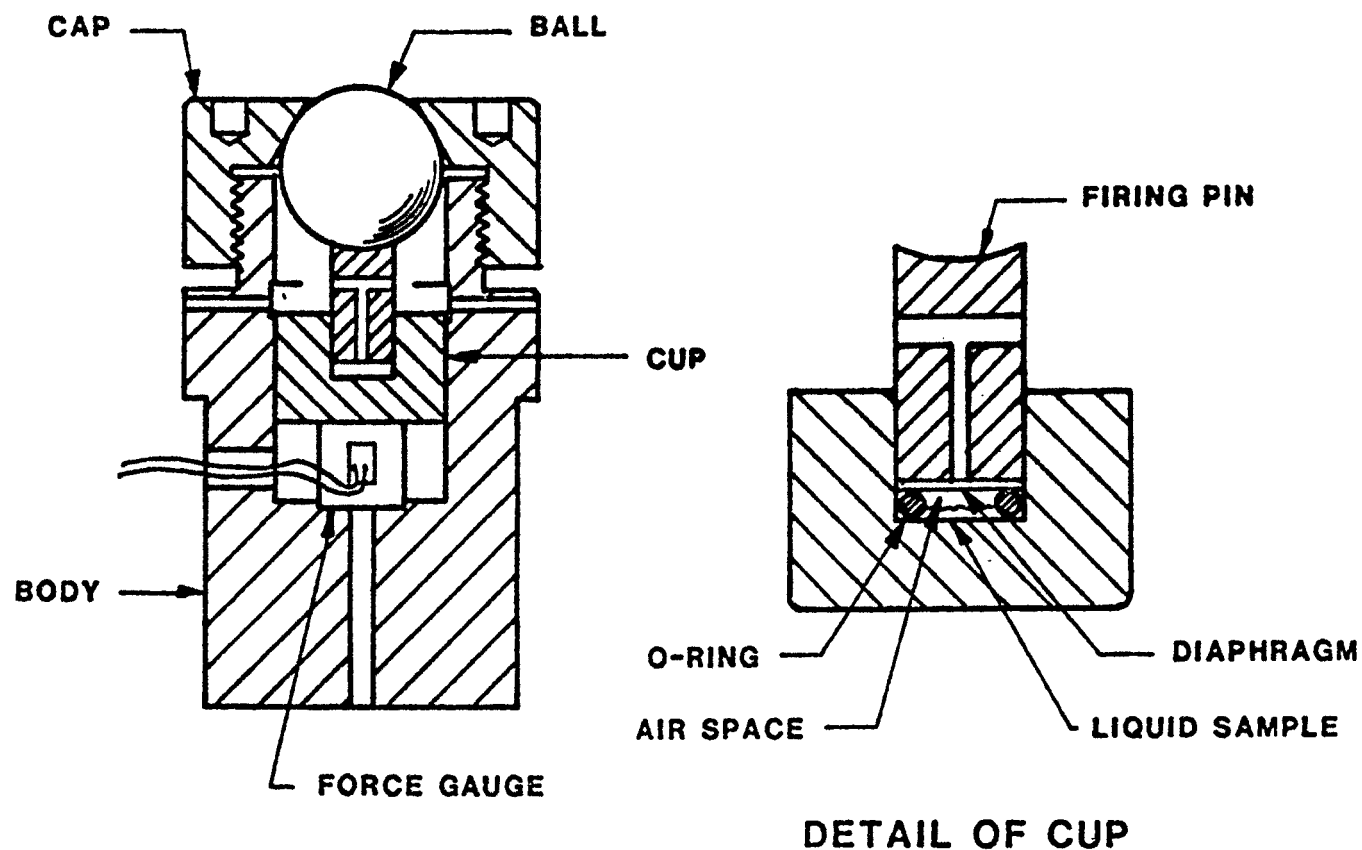


Figure 6, Experimental arrangement for ASTM impact test.

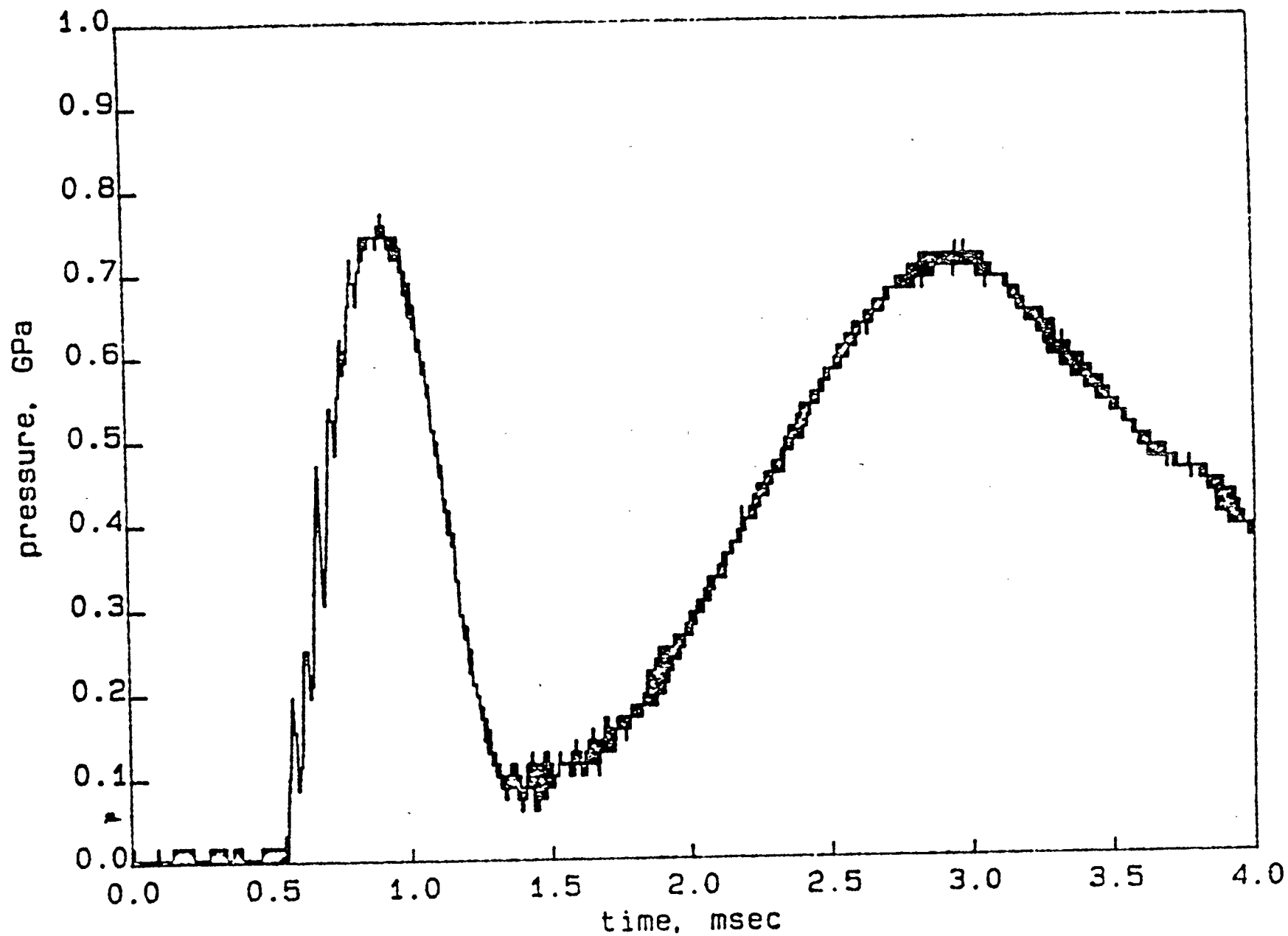


Figure 7, Pressure records from ASTM impact test on a EGMN based explosive.

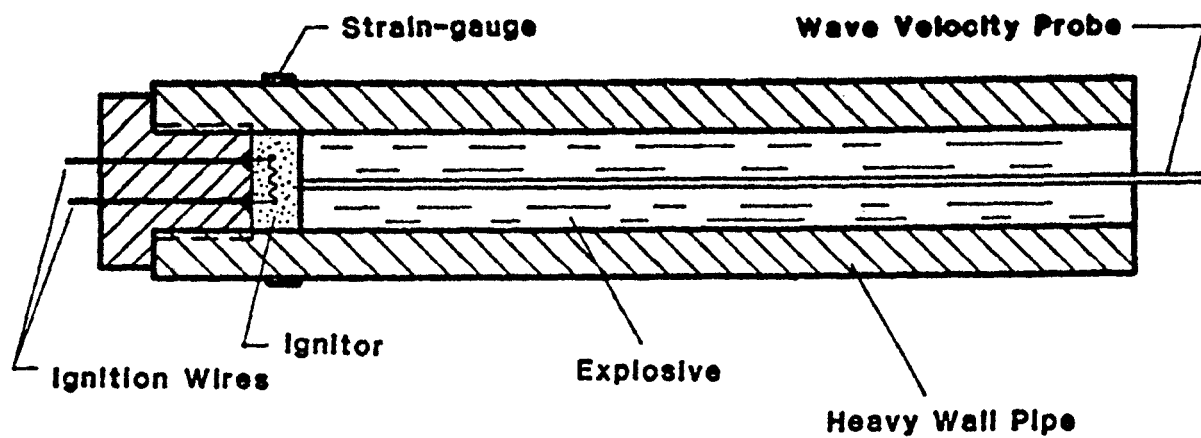


Figure 8, Schematics of experimental set up of DDT test.

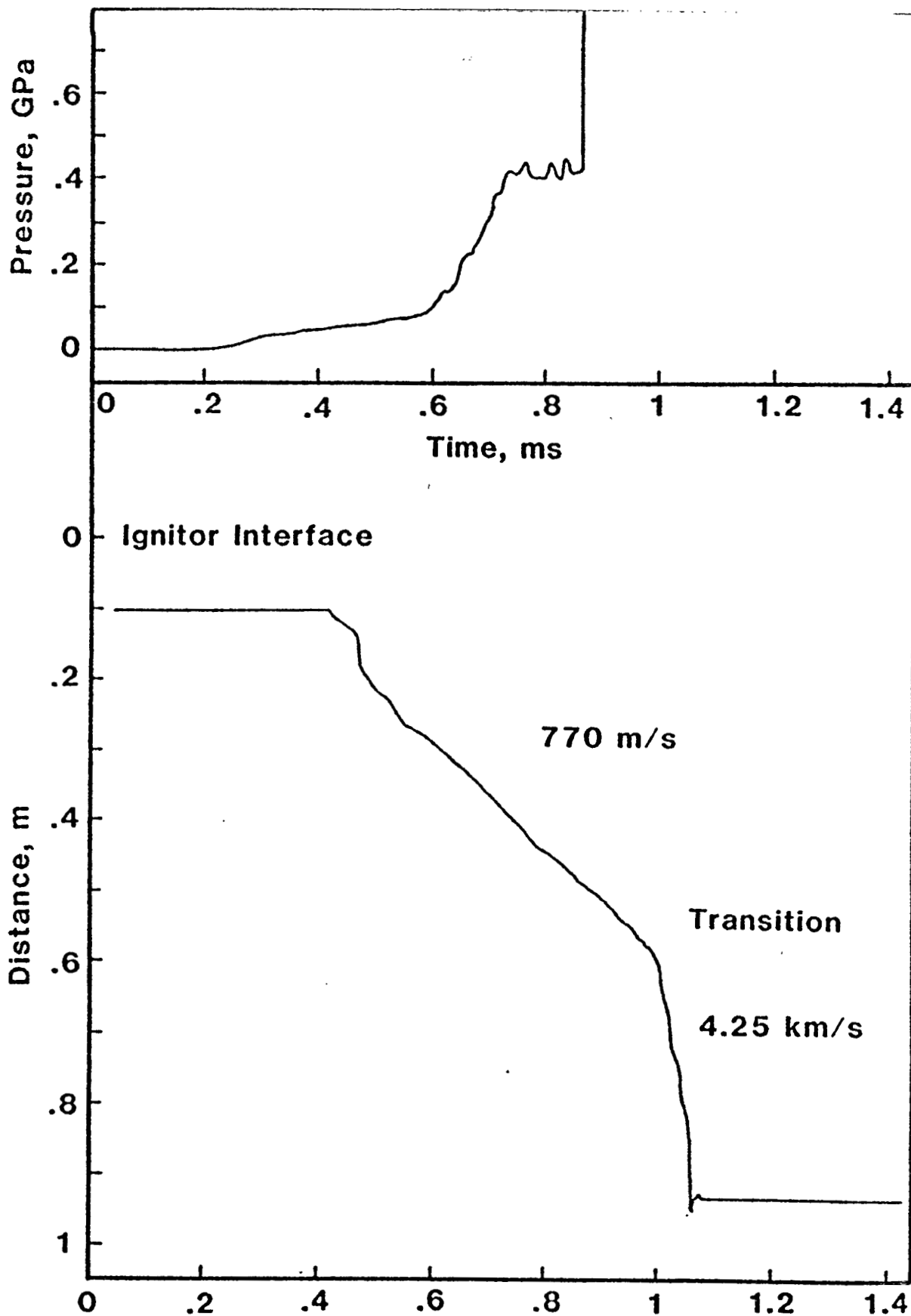


Figure 9,

Ignition end pressure and wave velocity records for a test with EXP-A initiated with RDX/black powder igniter.

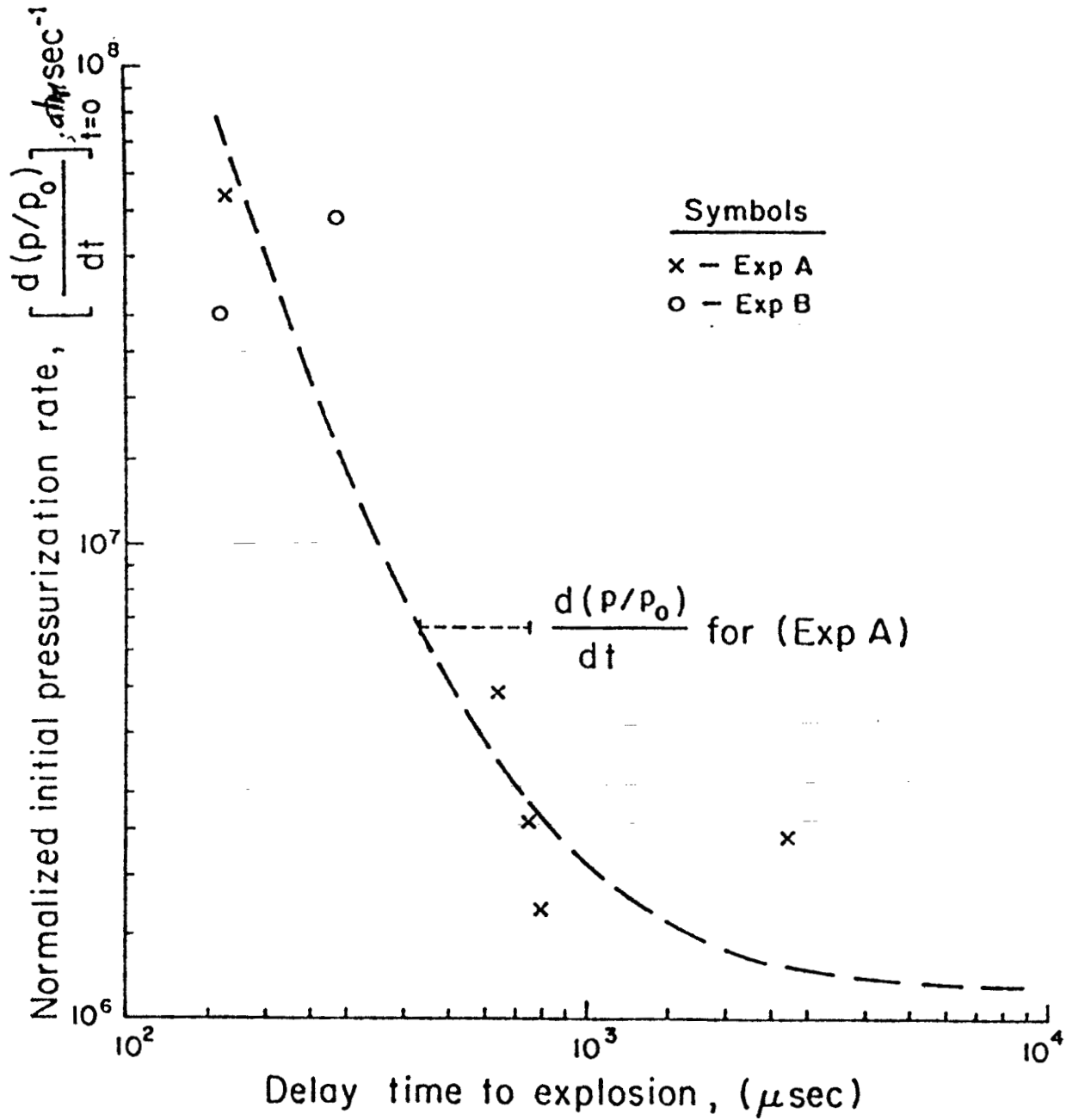


Figure 10, Correlation of the pressurization rate with the delay time to explosion.